IOP Conf. Series: Materials Science and Engineering **118** (2016) 012021 doi:10.1088/1757-899X/118/1/012021

Graded High-Strength Spring-Steels by a Special Inductive Heat Treatment

A Tump[1,2] and R Brandt[2]

[1] Mubea Fahrwerksfedern GmbH, Dr.-Karl-Heinz-Muhr-Straße , 99631 Weißensee, Germany
[2] Lehrstuhl für Werkstoffsysteme für den Fahrzeugleichtbau, Universität Siegen – Fakultät IV, Am Eichenhang 50, 57076 Siegen, Germany

Abstract. A method for effective lightweight design is the use of materials with high specific strength. As materials e.g. titanium are very expensive, steel is still the most important material for manufacturing automotive components. Steel is cost efficient, easy to recycle and its tensile strength easily exceeds 2,000 MPa by means of modern QT-technology (Quenched and Tempered). Therefore, lightweight design is still feasible in spite of the high density of steel. However, a further increase of tensile strength is limited, especially due to an increasing notch sensitivity and exposure to a corrosive environment. One solution is a special QT-process for steel, which creates a hardness gradient from the surface to the core of the material. This type of tailored material possesses a softer layer, which improves material properties such as fracture toughness and notch sensitivity. This leads to a better resistance to stress corrosion cracking and corrosion fatigue. Due to this optimization, a weight reduction is feasible without the use of expensive alloying elements. To understand the damage mechanism a comprehensive testing procedure was performed on homogeneous and gradient steels. Some results regarding the fracture mechanic behavior of such steels will be discussed.

1. Introduction

The application of materials with a high specific strength is a common method to reduce the weight of components that demand a high fatigue strength. Thus, high-strength steels are still important for the manufacturing of automotive components. Steel is cost efficient, easy to procure and easily recyclable compared to other lightweight-materials, e.g. titanium. Steel can have a tensile strength of more than 2,000 MPa that allows components to be designed with considerable weight reduction. However, the use of a high-strength steel requires a certain corrosion protection for components when they are exposed to a corrosive environment.

Alloying elements like Ni, V, Nb, Ti, W or Cu [1], [2], [3] are applied in order to increase the fatigue limit of steels. These elements are able to increase the toughness (Ni), to refine the grain size (V, Nb, Ti), and enhance the corrosion resistance (Cu) [3]. Furthermore, the fatigue limit is enhanced by means of casehardening, nitrating or carburizing [4]. However, increasing the hardness leads to a decrease in ductility, an increase in notch sensitivity [5], [6] as well as the hydrogen embrittlement sensitivity [7]. A new approach is the SLM-technology (Surface Layer Modification) for coil springs that increases the fatigue strength of high-strength spring steels which are exposed to a corrosive environment [8]. The SLM-technology aims to reduce the hardness within a thin surface layer of the spring wire, thus leading to a graded material, which exhibits a locally increased notch sensitivity and corrosion resistance [6].

For a better understanding of the microstructural mechanisms, a fracture mechanical investigation was conducted for homogeneously hardened as well as graded specimens.

2. Characterization of the material

For this study, a standard spring steel (54SiCr6) was used. Its composition is given in Table 1.

Table 1. Chemical composition of 54SiCr6 (arithmetic mean out of three specimen)

C	Si	Mn	P	S	Cu	Al	Cr	Ni	V	As
0.535	1.400	0.700	0.008	0.005	0.050	0.023	0.250	0.125	0.005	0.005

The initial wire rod diameter of d_{wire} = 20 mm was firstly reduced to d_{wire} = 17 mm by means of a drawing process. Then the drawn rod was tested for local cracks and hole-like flaws in both longitudinal and transverse direction by means of eddy current inspection (Circograph® and Defectomat® from the Institute Dr. Foerster GmbH & Co. KG).

The drawn wire was then inductively heated at a temperature of 900 °C and subsequently water quenched to room temperature. Finally the hardened wire was tempered at different temperatures (minimum 400 °C) in order to have five types of specimens with different tensile strengths ranging from R_m = 1,700 MPa to R_m = 2,200 MPa. The samples to be graded, representing the SLM technology, were treated by an additional inductive heating procedure (Figure 1) within the tempering unit in such a way that an overall tensile strength of R_m = 2,000 MPa was reached.

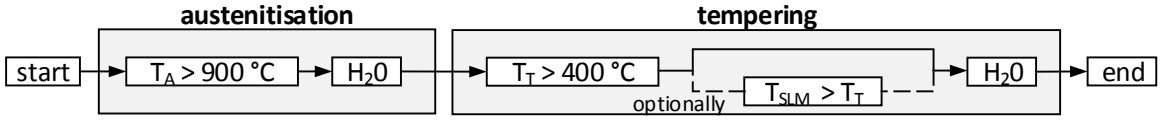

Figure 1. Schematic heat treatment process for homogeneous and gradient wire

The resulting martensitic structure contained retained austenite < 4 % (measured with X-ray diffractometer D8 Advance™ from Bruker Corporation). The prior austenite grain size was approximately 10 µm (Table 2).

All four-point-bending specimen (SENB – Single Edge Notched Beam) for fracture mechanical testing were milled and ground out of the QT-wire. Finally, the notches were eroded (Figure 2 – a, b) to a depth of 1.5 mm.

The crack propagation rates da/dN were measured according to ASTM E 647–08 [9].

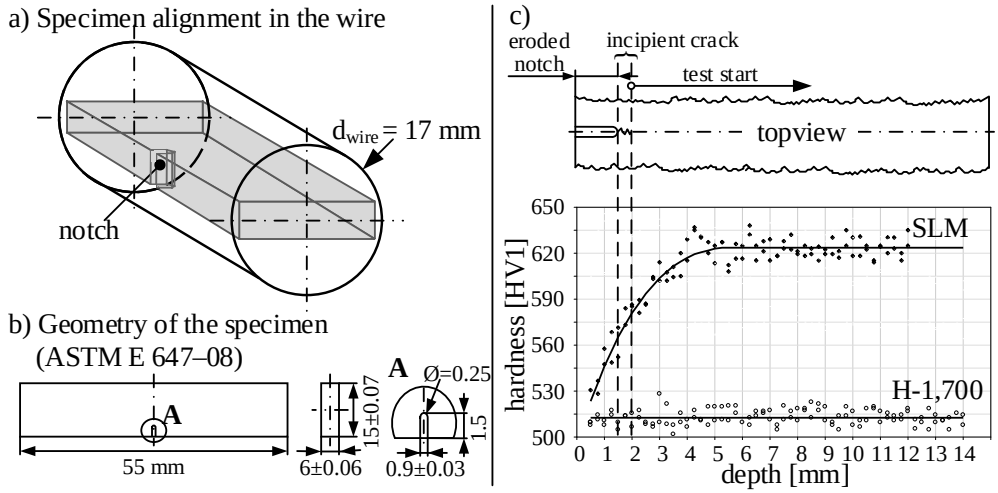

Figure 2.a) Specimen position in the wire, b) Geometry of the specimen, c) characteristic hardness profile of the graded material (SLM) and in comparison to the homogeneous material H-1,700

The graded material exhibits a characteristic hardness profile (Figure 2 - c). At the surface the hardness is 530 HV1, and it steadily increases up to 620 HV1 at a depth of approximately 5 mm. From there on the hardness remains constant.

The average material properties, like tensile strength R_m, yield strength $R_{p0.2}$, reduction of area Z, Vickers hardness HV1 and grain size class G of all tested specimens are listed in Table 2.

Table 2. Material properties of the tested specimen

Material	**tensile test wire [a] [MPa]**			**hardness SENB [b] [HV1]**			**ASTM grain size number [b]**	
	R_m	$R_{P0.2}$	Z	surface [c]	core [d]	integral	surface [c]	core [e]
1. H-1,700	1,690	1,462	46		512		G11.0	G11.0
2. H-1,900	1,876	1,633	43		573		G10.5	G10.0
3. H-2,000	1,980	1,717	41		605		G11.0	G11.0
4. H-2,100	2,091	1,810	31		635		G11.0	G10.5
5. H-2,200	2,207	1,894	24		664		G10.5	G10.5
6. SLM	2,022	1,735	45	581	623	615	G11.0	G10.5

[a] arithmetic mean out of five specimens
[b] arithmetic mean of three specimens
[c] distance from the surface = 2 mm
[d] distance from the surface = 5–15 mm
[e] depth from the surface = 7.5 mm

3. Fracture mechanical testing method

The tests were performed at a constant stress ratio of R = 0.2 with a test frequency of f = 120 Hz using a resonant testing machine (Cracktronik with Fractomat from Russenberger Prüfmaschinen AG). Sharp starting cracks were established at a stress intensity level of $\Delta K = 18$ MPa$\sqrt{m}$. The crack length was measured with crack measuring films by indirectly measuring the change in electrical resistance. The fracture-analysis were performed by means of scanning electron microscopy (Sigma 300 from Carl Zeiss Microscopy GmbH).

4. Results

The characterization of stable crack growth is commonly described by the Paris-Erdogan-Law (1).

$$\frac{da}{dN} = C \cdot (K)^m \tag{1}$$

In order to determine the Paris-parameters (C and m) at least three specimens of each material were tested. Using the measurement points of all samples the corresponding regression curves were calculated by means of Gauß'least square method.

All Paris-Erdogan-law curves measured, representing the stable crack growth behavior of the materials with different hardness levels and profiles, are shown in Figure 3. Considering the homogeneously hardened and tempered materials, it becomes clear that the crack growth rate increases corresponding to the increase of the material hardness level.

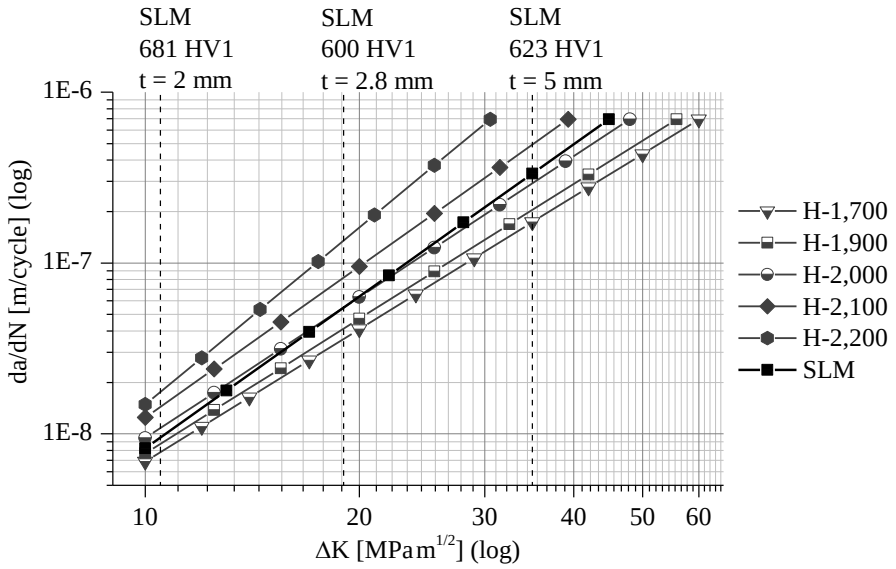

Figure 3. Regression curves for each material in the state of stable crack propagation

It is obvious that the curves are shifted upwards with increasing material hardness and the gradient becomes steeper, too (Figure 3). The numerical values of the Paris-Erdogan-law parameter C and m are given in the table of figure (Figure 4. – b).

a)

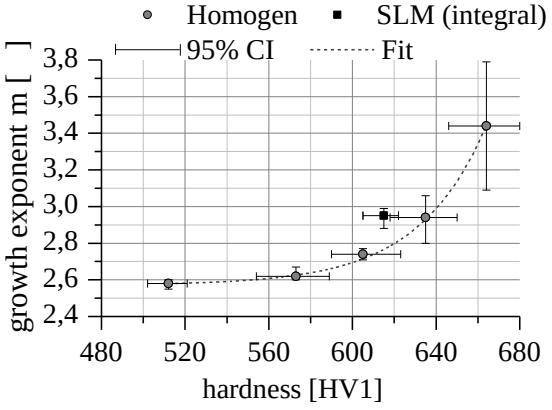

b)

material	m	C	R^2 [%]	s
H-1,700	2.58	1.81E-11	96.1	0.14
H-1,900	2.62	1.85E-11	96.0	0.14
H-2,000	2.74	1.72E-11	94.8	0.19
H-2,100	2.94	1.44E-11	75.4	0.23
H-2,200	3.44	5.39E-12	68.9	0.16
SLM	2.95	9.15E-12	95.7	0.14

with: R^2: coefficient of determination
s: standard deviation
CI: confidence interval

Figure 4. a) Relation between the hardness and the Paris-Parameter m, b) Paris-Erdogan-law parameters of the different materials

For a better understanding of the change of the growth exponent m with the hardness of the material, the growth rate is plotted vs. the hardness in Figure 4a). At comparatively low hardness levels of 510 HV1 to almost 600 HV1 only a minor increase of m is discovered. However, as soon as the hardness exceeds a level of 600 HV1 the growth exponent m shows a considerable increase with materials hardness. Compared to the homogeneous material, the graded material has a growth exponent value of m = 2.95 which is close to the value of the homogenously hardened material H-2,100. A corresponding symbol for SLM, at its integral hardness, is also plotted in the diagram (Figure 4. – a). It is clearly located above the curve representing the homogeneous materials which means that the gradient is higher. However, the site of the Paris-Erdogan-law curve of SLM lies significantly below the curve representing H-2,100 (Figure 2.).

The fractography of the fractured SLM specimens discloses that homogeneously hardened and tempered materials up to a hardness of ≈ 575 HV1 shows a transcrystalline fracture surface (Figure 5. – a). At a magnification of 2,500 individual striations with a spacing of nearly 1 µm are visible (Figure 5. – a.2).

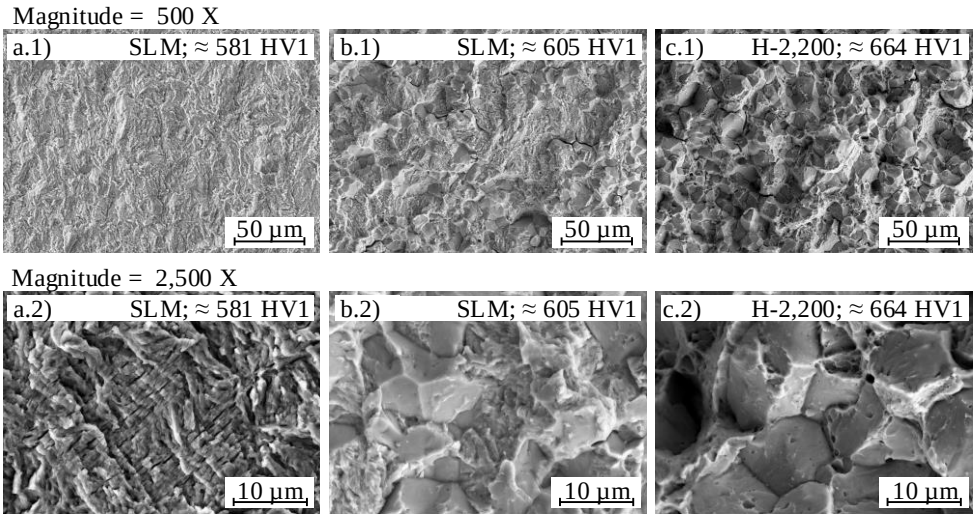

Figure 5 a) Transcrystalline striations at 581 HV1 (SLM-specimen), b) Mixed fracture patterns of striations and intercrystalline fracture at 605 HV1 (SLM-specimen), c) Nearly complete intercrystalline fracture at 664 HV1 (H-2000-specimen)

The portion of intercrystalline fracture sites increases as the cracks becomes longer, i.e. the core material becomes harder. More and more intercrystalline fracture sites occur in the range of 575 HV1 to 628 HV1 and intercrystalline fracture clearly dominates at a hardness level beyond 628 HV1 (Figure 5. – c.).

5. Discussion and concluding remarks

Stable crack propagation of high strength spring steels were investigated and it can be concluded that the crack propagation rate accelerates with increasing tensile strength and increasing hardness, respectively. This result is not unexpected because the ductility decreases with higher tensile strength and similar results can be found in the literature [5]. In contrast to the results reported here indicate not only a mere shift of the Paris-Erdogan-curve but also a change in gradient (Figure 3) which becomes evident by plotting the growth exponent m vs. the material hardness (Figure 4 – a). One hint to the source of the changing gradient was found in the study of the patterns of the fracture surface. The fracture patterns show a change from transcrystalline striations, with a spacing of approximately 1 µm between them, to a nearly pure intercrystalline state with increasing hardness (Figure 5).

Furthermore a method for a fracture mechanical testing procedure for SLM material has been developed. By means of this method, it was possible to analyze different phases of crack growth within a graded material. The crack propagation rate of the graded material is "slow" in the beginning, similar to the rate of the homogeneous material H-1,900. This can be understood by comparing the local SLM-hardness (581 HV1) at a depth of 2 mm (Figure 2 – c) with the average hardness of H-1,900 (573 HV1). The continuously increasing hardness of SLM with increasing crack length leads to a faster increase of the crack propagation rate. At a crack-length of 2.8 mm the crack propagation rate is still below that of the material H-2,000 which has approximately the same tensile strength or the same integral hardness, respectively (Table 2). This implies that SLM-technology can delay the time to failure, considering cracks starting from the material surface or from inclusions within a surface layer of 2.8 mm thickness.

Overall, the gradient steel was subject to fracture mechanical testing under dry conditions and the crack propagation behavior could be characterized. The effect of a corrosive environment was not taken into account and will be a subject for future investigations

Acknowledgements
Special thanks to the "Lehrstuhl für Materialkunde und Werkstoffprüfung" of the University of Siegen for conducting the fracture mechanical tests and to the "Europäischer Fonds für regionale Entwicklung" (EFRE) for the financial support.

Literature

[1] Masumoto K.; Kaiso M.; Ibaraki N.: Developments of Ultra-high Strength Wire Rods for Valve Springs with Excellent Fatigue Life, Kobe Steel Engineering Reports 2009 – Band 59 Heft 1, pp.67-70, 2009

[2] Perrad F.; Charvieux F., Languillaume J.: A new spring steel with improved ductility dedicated for high strength parabolic leaf springs, 2nd International Conference Super-High Strength Steels, Associazione Italiana di Metallurgia (AIM), 2010

[3] Perrad F.; Mendibide C.; Yoshihara N.; Namimura Y.; Ibaraki N.: High strength spring steels with improved ductility and corrosion resistance, International Conference on Steels in Cars and Trucks (SCT), pp. 106-113, Stahleisen GmbH, 2008

[4] Nishimura T.; Hagiwara Y.; Yamada K.; Ozone T.; Itoh Y.; Hayashi H.; Homma S., The Valve Springs Carbo-Nitrided at High Temperature for High Speed Engines; SAE Technical – Paper Series, no. 890777, 1989, ISSN 0148-7191,

[5] Tange A.; Akuto T.; Takamura N.: Relation between shot-peening residual stress distribution and fatigue crack propagation life in spring steel, Transactions of Japan Society of Spring Engineers – Vol. 1991 No. 36, pp. 47–53, NHK Spring Co.,Ltd., 2010

[6] Tump A.; Brandt R.; Klapprott S.: Gradientenstahl für Achsfedern, Tagungsband des Ilmenauer Federntags; 2013

[7] Kobayashi K.; Yamahuchi A.; Komazaki S.-i.; Misawa T.; Kohno Y.; Fukuzumi T.: Effekt of tensile strength on pitting corrosion resistance and hydrogen desorption profile in automobile spring steels, 11th International Congress on Fracture, 2005

[8] Neubrand J.; Hartwig M.; Patent term – DE 10 2009 011 118 A1, Muhr und Bender KG, 2010

[9] ASTM E 647–08, Standard Test Method for Measurement of Fatigue Crack Growth Rates, ASTM International